



# IPN beads prepared by tailoring of cassia tora gum and sodium carboxymethyl cellulose using $Al^{+++}$ for controlled drug delivery

Alka Lohani <sup>a,\*</sup>, Mohit Maurya <sup>a</sup>, Sushil Kumar <sup>a</sup>, Navneet Verma <sup>b</sup>

<sup>a</sup> School of Pharmaceutical Sciences, IFTM University, Moradabad, Uttar Pradesh, 244102, India

<sup>b</sup> Pharmacy Academy, IFTM University, Moradabad, Uttar Pradesh, 244102, India

## ARTICLE INFO

### Keywords:

Interpenetrating polymeric network  
Controlled release  
Sodium carboxymethyl cellulose  
Cassia tora gum

## ABSTRACT

In the present research, the development of pH-sensitive IPN (interpenetrating polymeric network) beads made of cassia tora gum, sodium carboxymethyl cellulose, and trivalent ions, as well as their applicability for controlled release of diclofenac sodium (DFS), is discussed. The prepared IPN beads were characterized by FTIR, DSC, XRD and SEM analysis and tested for size, drug encapsulation efficiency, swelling behavior, and drug release. The influence of several factors, including polymer ratio, gelation time, and crosslinker concentration, on the physicochemical properties and rate of drug release from the IPN beads was studied. The production yield of IPN beads was found to be in the range of 89.36%–92.76%. FTIR analysis confirmed the stability of the drug in the IPN matrix. The results of DSC and XRD analysis revealed that the drug was present in crystalline form in the interpenetrating polymer matrix. The IPN beads were nearly spherical in shape and ranged in size from  $215 \pm 0.14$  to  $485 \pm 0.20$   $\mu\text{m}$ . The drug entrapment efficiency was found to be in the range of  $79.50 \pm 1.69\%$  to  $91.42 \pm 1.99\%$ . The swelling ability of IPN beads was found to be low in acidic media and high in alkaline media. The swelling efficiency ranged from  $122.34 \pm 1.22\%$  to  $210.56 \pm 1.04\%$  in acidic pH (1.2) and from  $299.16 \pm 1.80\%$  to  $518.34 \pm 1.98\%$  at higher pH (7.4). In acidic pH, IPN beads showed extremely low drug release but a relatively high and sustained drug release profile in alkaline pH. The results of the study suggest that DFS-loaded IPN beads might be utilized to reduce the release of drug in acidic pH and modify the release in alkaline pH, which might reduce the stomach-related side effects of DFS.

## 1. Introduction

Over the past few decades, polymers, the most adaptable class of materials, have altered our daily lives. A technical progress in the development of innovative drug-delivery systems resulted from the merging of pharmaceutical and polymer sciences [1,2]. Polymers have facilitated the development of such drug delivery systems by allowing therapeutic agents to be released in a controlled manner over an extended period of time, delivering active pharmaceutical ingredients (APIs) to the specific sites, and improving the stability of hydrophilic and hydrophobic drugs. To improve the *in vivo* behavior of dosage forms, selection of right polymer is very crucial. The choice of polymer can, to a certain extent, regulate disintegration of the dosage form, release of the drug from the dosage form, dissolution, absorption, and bioavailability [3]. In order to formulate the customized drug delivery system, polymers can be used individually or in combination. In recent years, the development of polymer blends has been aided by an ever-increasing

need for superior polymer qualities for the formulation of different drug delivery systems [4]. One of such examples is the “Interpenetrating Polymer Network” (IPN), which is built on combining natural and/or synthetic polymers, either alone or in combinations. When two polymer species are combined, the network built by the first polymeric system gets entangled with the polymer chains of the second system, and the resulting polymer mixture creates a network that is physically cross-linked [5]. Each polymer network in the IPN system maintains its unique characteristics, allowing for synergistic improvements in strength or toughness [6]. IPNs have outperformed traditional individual polymers, and as a result, the applications for this smart class of polymers have expanded quickly [7]. These polymeric systems have shown promise in drug delivery, particularly in applications needing controlled release.

Natural polysaccharide gums are one of the most widely used industrial raw materials for drug delivery systems due to their sustainability, biodegradability, and biosafety. Due to their availability, low

\* Corresponding author.

E-mail address: [alkalohani06@gmail.com](mailto:alkalohani06@gmail.com) (A. Lohani).

<https://doi.org/10.1016/j.jddst.2023.104308>

Received 1 November 2022; Received in revised form 10 February 2023; Accepted 23 February 2023

Available online 24 February 2023

1773-2247/© 2023 Elsevier B.V. All rights reserved.

cost, and lack of toxicity, natural gums are favoured over synthetic alternatives. Most of the natural gums are used as food additives or drug delivery systems and are safe for oral consumption. Cassia tora gum is one of the natural polysaccharides extensively used as a food additive. Cassia tora gum (CTG) is obtained from the seeds of *Cassia tora* Linn (Family-Leguminosae). It is an annual herbaceous weed that is widely distributed in India [8]. Seed gums, also referred to as seed galactomannans, are significant food hydrocolloids utilized in the pharmaceutical, cosmetics and food industries [9]. CTG can be used to formulate various pharmaceutical dosage forms for controlled/sustained drug release systems because of its outstanding emulsifying, stabilizing, binding, thickening, suspending and water-retention abilities [10].

Sodium carboxymethyl cellulose (SCMC), a cellulose derivative and an anionic cellulose derivative that is widely employed in a various industry due to its unique emulsifying, suspending, thickening, adhesion, film-forming, water retention and high acid resistance capabilities [11, 12].

According to a study, trivalent metal ions perform much better as a crosslinker than divalent metal ions because they crosslink faster due to their higher valency. Furthermore, the study found that beads cross-linked with trivalent metal ions released the API in simulated intestinal fluid for an extended time duration than those cross-linked with divalent metal ions [13]. Due to this, trivalent  $Al^{+++}$  ions were employed in this study to produce IPN beads for extended intestinal-specific administration of diclofenac sodium (DFS).

DFS was used as a model drug in the present investigation. DFS is an effective non-steroidal anti-inflammatory drug that is clinically utilized to treat inflammation-induced pain, such as arthritis pain [14]. DFS has a biological half-life of between 1 and 3 h [15], hence frequent dosing is needed to keep the therapeutic drug level in the blood. The solubility of DFS is poor in acidic pH and at alkaline pH it solubilizes rapidly [16]. If present in the gastrointestinal tract in large dose, DFS might lead to stomach ulcers [17]. Therefore, an effort to formulate a delayed release delivery system of DFS can reduce side effects in the gastrointestinal environment, reduces the need of repeated dosing and enhance patient compliance.

The objective of this research work was to formulate DFS encapsulated IPN beads made up of combining two polymers (CTG and SCMC) using  $AlCl_3$  as a crosslinking agent. The prepared IPN beads will be tested for size, shape and surface morphology, drug encapsulation efficiency, swelling behavior and drug release from IPN beads.

## 2. Experimental

### 2.1. Materials

DFS was purchased from Central Drug House (P) Ltd. New Delhi, India (purity-98.5%). CTG (10,000cps (1%); Brookfield. Spindle No. 7, 20 RPM at 25 °C) was received from Sarda Gums and Chemicals, Rajasthan, India as a gift sample. SCMC (3000–5000 mPa (2%) at 20 °C) and calcium chloride, barium chloride, aluminium chloride, ferric chloride, zinc chloride was purchased from Hi-Media Laboratories Pvt. Ltd., Mumbai, India. All the chemicals used were of analytical grade.

## 3. Method

### 3.1. Preliminary trials for IPN bead formulation

Blank (placebo) IPN beads were made by varying the ratios of polymers (CTG and SCMC), and the concentration of crosslinking agent. First, an aqueous solution of CTG and SCMC was prepared. The resulting polymeric blend was dropped into a slightly agitated aqueous solution of the crosslinker using a hypodermic needle (21-gauge flat-tipped). In the preliminary stage, the salts  $Mg^{++}$ ,  $Ca^{++}$ ,  $Cu^{++}$ ,  $Ba^{++}$ ,  $Cd^{++}$ ,  $Co^{++}$ ,  $Zn^{++}$ ,  $Al^{+++}$  and  $Fe^{+++}$  (as chlorides) were used as crosslinking agents at

concentrations between 4 and 6% w/v, and their capacity to produce strong, spherical, and separable beads was assessed. It was seen that in the presence of  $AlCl_3$  ions, the IPN beads were formed properly in comparison to other crosslinkers used. The prepared beads were separated by filtration and dried at 40 °C.

### 3.2. Formulation of drug loaded IPN beads

DFS loaded IPN beads were prepared by an ionotropic gelation technique using  $AlCl_3$  as a crosslinker (Fig. 1) [18]. To begin, an aqueous homogeneous solution of polymers (CTG and SCMC) was prepared, and the drug (DFS) was dispersed into it with continuous stirring in a magnetic stirrer at a low speed (50 rpm) to avoid air bubble entrapment. In a separate beaker, the required amount of  $AlCl_3$  was dissolved in water. Using a flat-tipped hypodermic needle (21 gauge), the prepared dispersion of drug and polymers was dropped into an aqueous solution of  $AlCl_3$  that had been gently agitated using a magnetic stirrer. The prepared IPN beads were allowed to incubate in the crosslinker solution for 30 or 60 min (gelation time). After that, the IPN beads were filtered and washed 2–3 times with distilled water and then allowed to dry at 40 °C in hot air oven. Table-1 represents the formulation composition of prepared IPN beads.

Following variable were considered while preparing the IPN beads-

- 1 The polymer concentration was kept constant at 3% w/v.
- 2 The ratio of CTG to SCMC was altered.
- 3 The concentration of the crosslinking agent varied from 4 to 6% w/v.
- 4 The gelation time in the crosslinker solution ranged from 30 to 60 min.

## 4. Analytical methods

### 4.1. Fourier transform infrared (FTIR) spectroscopy

The FTIR spectra of DFS, placebo IPN beads and DFS loaded IPN beads were taken by Shimadzu FTIR-Spectrophotometer (Model FTIR-8400S, Shimadzu, Japan) using KBr pellets. DFS/placebo/drug loaded IPN beads were crushed and combined with KBr and converted into the pellet separately at 100 kg pressure by using the hydraulic press pellet technique. The FTIR spectra was recorded in a region of 400–4000  $cm^{-1}$ .

### 4.2. Differential scanning calorimetry (DSC) analysis

A Differential Scanning Calorimeter (Perkin-Elmer instrument, Pyris-Diamond TG/DTA, Singapore) was used to record the DSC thermogram of the DFS, polymers, placebo IPN beads and drug-loaded IPN beads. The DSC thermogram was recorded at a heating rate of 10.00 °C/min, and a heating range of 30.00 °C–440.00 °C.

### 4.3. X-ray diffraction (XRD) analysis

XRD analysis of DFS, placebo IPN beads and drug-loaded IPN beads was done with the help of an X-ray diffractometer (Model: D/Max 2200, Rigaku Corporation, Japan). The samples were scanned from 0 to 50 °C at a diffraction angle of  $2\theta$  using a Ni-filtered  $Cu-K\alpha$  ( $\lambda = 1.54$ ) radiation source, a current of 30 mA, a voltage of 40 kV, and a scan speed of 5°/min.

### 4.4. Size of IPN beads

An optical microscope was used to measure the size of IPN beads. The eyepiece micrometer was calibrated using a standard stage micrometer. The IPN beads were kept on a glass slide, the number of divisions of the calibrated eyepiece was counted, and lastly, the individual particle diameter was determined [18]. 200 beads were randomly selected and mean particle diameter was determined.

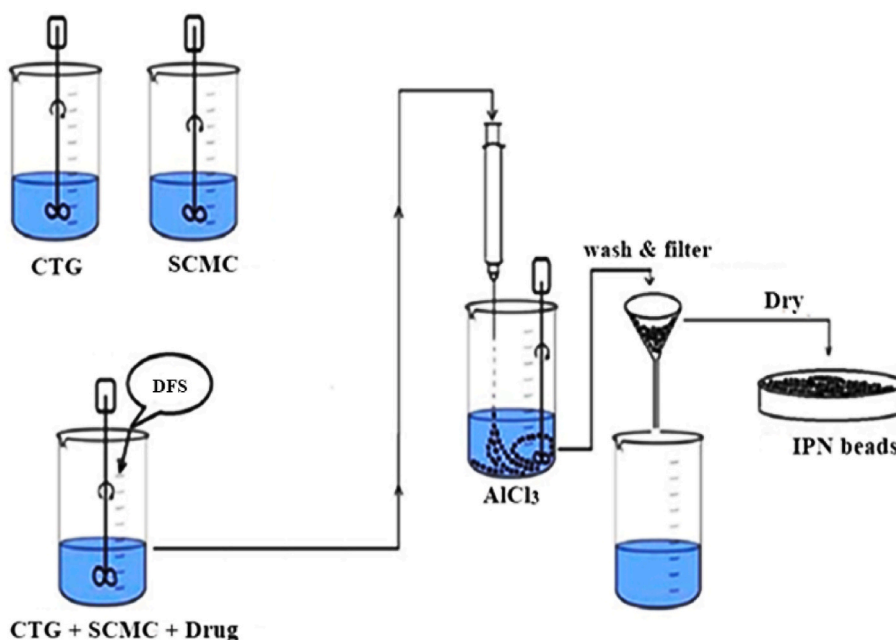


Fig. 1. Graphical representation of IPN beads formulation.

**Table 1**  
Composition of the DFS loaded IPN beads.

Code	Polymer Ratio (CTG: SCMC) (%) w/v	Drug loading <sup>a</sup> (%) w/w	Concentration of AlCl <sub>3</sub> (%w/v)	Gelation time (min)
A1	1:1	30	4	30
A2	1:1.5	30	4	30
A3	1:2	30	4	30
A4	1:1	30	6	30
A5	1:1.5	30	6	30
A6	1:2	30	6	30
A7	1:1	30	6	60
A8	1:1.5	30	6	60
A9	1:2	30	6	60

<sup>a</sup> (% w/w of total polymer).

#### 4.5. Scanning electron microscopy (SEM)

Scanning Electron Microscopy (SEM) examination reveals details about the IPN beads, such as their shape and exterior morphology (surface texture). The SEM analysis was performed by a scanning electron microscope (JEOL India Pvt Ltd; Model: JEOL JSM 7610f) at low ( $\times 55$ ) and high ( $\times 1800$ ) magnifications at an acceleration voltage of 5.0Kv.

#### 4.6. Production yield of IPN beads

The production yield of prepared IPN beads was determined with the help of the total amount of polymers (CT and SCMC) and drug used for the preparation of IPN beads. Production yield (%) was calculated with the help of the following formula [19]:

$$\text{Production yield (\%)} = \frac{\text{Total amount of prepared IPN beads}}{\text{Amount of drug + total amount of polymers used}} \times 100$$

#### 4.7. Drug entrapment efficiency

50 mg of dried drug-loaded IPN beads were accurately weighed and crushed in a glass mortar with a pestle. The crushed beads were added to 50 ml phosphate buffer (pH 7.4). This mixture was stirred on a magnetic

stirrer (50 rpm) for 6 h and then filtered. The filtered sample was analyzed by a UV-Visible spectrophotometer at 277 nm. The drug entrapment efficiency (%) was calculated by the following formula [20]:

$$\text{Drug entrapment efficiency (\%)} = \frac{\text{Experimental drug content}}{\text{Theoretical drug content}} \times 100$$

#### 4.8. Swelling behaviour of IPN beads

The swelling behaviour of prepared IPN beads was observed in acidic medium (pH 1.2) and basic medium (phosphate buffer; pH 7.4). 100 mg IPN beads were taken and allowed to swell in the medium (50 ml) separately at 37 °C for 12 h. After that, the swollen IPN beads were filtered, the adhered liquid was blotted gently with the help of soft tissue paper and the weight of the swollen IPN beads was noted. The swelling efficiency was determined by applying the following formula [19].

$$\text{Swelling (\%)} = \frac{\text{mass of swollen beads} - \text{mass of dry beads}}{\text{mass of dry beads}} \times 100$$

#### 4.9. Drug release, kinetics and mechanism study

*In-vitro* drug release study was performed by using Basket type dissolution apparatus (USP Apparatus I) (Electro Lab TDT-08, Mumbai, India). Drug release from prepared IPN beads was analyzed in gastric condition i.e., at pH 1.2 for initial 2 h and then at pH 7.4. Drug loaded IPN beads (equivalent to 50 mg of drug) were placed in dissolution media (900 ml; 37 ± 0.5 °C) and the paddle was rotated (50 rpm). At regular time intervals, a 5 ml sample aliquot was taken out and the same volume of fresh medium was added right away. The withdrawn aliquots were examined using a UV spectrophotometer (UV-1800, Shimadzu, Tokyo, Japan) at 277 nm.

The kinetics of drug release from IPN beads was studied using a number of empirical equations, including zero-order, first-order, Higuchi square root, and Korsmeyer-Peppas.

The dissolution profiles of all the formulations were also analyzed by calculating two factors, f1 (difference factor) and f2 (similarity factor). Factor f1 indicates the percentage difference (dissimilarity) between two dissolution profiles; factor f2 indicates the average percentage of similarity between two dissolution profiles. The values of fit factors (f1 and f2) are dependent on the number of sampling time points chosen. Ac-

According to FDA, the difference factor (f1) calculates the percent (%) difference between the two curves at each time point and is a measurement of the relative error between the two curves:

$$f1 = \left\{ \left[ \sum_{t=1}^n |R_t - T_t| \right] / \left[ \sum_{t=1}^n R_t \right] \right\} \times 100$$

The similarity factor (f2) is a logarithmic reciprocal square root transformation of the sum of squared error and is a measurement of the similarity in the percent (%) dissolution between the two curves.

$$f2 = 50 \times \log \left\{ \left[ 1 + \left( \frac{1}{n} \sum_{t=1}^n (R_t - T_t)^2 \right) \right]^{-0.5} \times 100 \right\}$$

where n is the number of dissolution intervals,  $R_t$  indicates the percentage release results of the reference at time point t, and  $T_t$  indicates the percentage release results of the test formulation at time t. Dissolution was performed by taking 12 units of each formulation.

## 5. Results and discussion

### 5.1. Capacity of metal ions to form isolatable discrete beads

In the preliminary stage, the salts  $Mg^{++}$ ,  $Ca^{++}$ ,  $Cu^{++}$ ,  $Ba^{++}$ ,  $Cd^{++}$ ,  $Co^{++}$ ,  $Zn^{++}$ ,  $Al^{+++}$  and  $Fe^{+++}$  (as chlorides) were used as crosslinking agents at concentrations between 4 and 6% w/v, and their capacity to produce strong, spherical, and separable beads was assessed.  $Mg^{++}$ ,  $Cu^{++}$  and  $Cd^{++}$  not even managed to form nascent IPN beads. Utilizing  $Ca^{++}$ ,  $Ba^{++}$ ,  $Co^{++}$  and  $Zn^{++}$ , IPN beads were initially visible when the polymeric blend solution was added; however, during the curing period, the beads did not become sufficiently rigid and failed to separate after filtration. In the case of trivalent metal ions ( $Fe^{+++}$  and  $Al^{+++}$ ), it was found that they require a very short span of time to produce spherical, rigid and separable IPN beads. It was observed that when  $Al^{+++}$  was used, the rigidity of IPN beads was high and their shape was almost spherical without tailing. This was further confirmed by a study that reported that trivalent metal ions crosslink much more quickly than divalent metal ions due to their higher valency [13]. Due to this, trivalent  $Al^{+++}$  ions were employed in this study to produce IPN beads for extended and site-specific drug release.

### 5.2. Formation of IPN beads

During the formulation, it was observed that the polymeric blend of CTG and SMC was able to gel in the presence of trivalent metal ions to form IPN beads (Fig. 2). This can be explained as follows: when both the polymers blend together, the polymeric chains become physically entangled with each other, and when this blend is added to the crosslinking solution, a tight helix-helix agglomeration is formed in the presence of trivalent metal ions, i.e.,  $Al^{+++}$ .

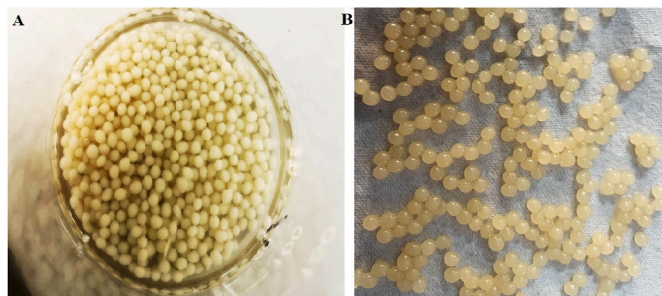


Fig. 2. Prepared IPN beads; A- IPN beads in crosslinker solution; B- IPN beads after filtration.

### 5.3. Fourier transform infrared (FTIR) spectroscopy

The development of an interpenetrating polymer network and the stability of DFS in the IPN was examined using FTIR study. Fig. 3 represents the FTIR spectrum of DFS (Fig. 3A), physical mixture of drug and polymers (Fig. 3B), placebo IPN beads (Fig. 3C), and DFS loaded IPN beads (Fig. 3D). The OH group from the absorbed water is responsible for the absorption bands at  $3257.28 \text{ cm}^{-1}$  and peak at  $3386.57 \text{ cm}^{-1}$  was due to the N-H stretching in the FTIR spectra of the DFS. The FTIR peak at  $1556.46 \text{ cm}^{-1}$  is due to the C=O stretching vibration for carbonyl groups, and the peaks observed at  $1468.83 \text{ cm}^{-1}$  and  $1498.28 \text{ cm}^{-1}$  represent the scissoring vibration of the  $CH_2$  group adjacent to the carbonyl. The C-O stretching and C-N stretching absorption, together with the C-H bend (in plane) from the aromatic ring, are all related to the doublet peak at  $1305.07 \text{ cm}^{-1}$  and  $1282.08 \text{ cm}^{-1}$ . The out-of-plane C-H bend is shown by the sharp peak at  $766.38 \text{ cm}^{-1}$  and  $746.98 \text{ cm}^{-1}$ . Because placebo beads do not contain drug, no DFS-specific peaks were observed in their FTIR spectra. The FTIR spectra of physical mixture (drug and polymers) as well as drug-loaded IPN beads were seen to have the majority of the distinctive peaks of the drug with only small variations in the selected peaks. The results of the FTIR analysis showed that the drug was compatible with the polymers used in the study.

### 5.4. Differential scanning calorimetry (DSC) analysis

The changes in crystallinity, melting point, and the possibility of a drug-polymer interaction are all determined by the DSC study. DSC analysis of DFS, CTG, SMC, placebo IPN beads and drug loaded IPN beads was done and shown in Figs. 4 and 5. DSC thermogram of DFS showed an endothermic peak at  $285.82 \text{ }^\circ\text{C}$  and an exothermic peak at  $289.14 \text{ }^\circ\text{C}$  (Fig. 4A). The DSC thermogram of CTG showed a broad endothermic peak at  $73.36 \text{ }^\circ\text{C}$ , probably related to the evaporation of water (Fig. 4B). DSC thermogram of SMC revealed an endothermic peak at  $62.81 \text{ }^\circ\text{C}$  that was likely caused by water evaporation and decomposed at  $290.46 \text{ }^\circ\text{C}$  with an exothermic peak (Fig. 4C). On the DSC thermogram of placebo IPN beads, two clear endothermic peaks at  $147.96 \text{ }^\circ\text{C}$  and  $194.65 \text{ }^\circ\text{C}$  were observed (Fig. 5D). These peaks may have become evident as a result of the formation of the IPN structure. The DSC thermogram of drug-loaded IPN beads (Fig. 5E) revealed a strong endothermic peak at  $286.82 \text{ }^\circ\text{C}$ , similar to the DSC thermogram of DFS. This observation suggests that the drug was present in the IPN structure in the crystalline form. No exothermic peak was seen in the DSC thermograms of drug-loaded IPN beads, which indicates that IPN is thermally more stable in comparison to the native polymers.

### 5.5. X-ray diffraction (XRD) analysis

Preferred crystal orientations, phases, structures, and several structural factors, including strain, crystallinity, medium grain size, and crystal fissures, are all revealed by X-ray diffraction investigation. XRD study of DFS, placebo IPN beads, and drug-loaded IPN beads was done in order to validate the physical condition of the drug in the IPN beads. The results are displayed in Fig. 6. The X-ray diffraction patterns of DFS (Fig. 6A) showed sharp peaks due to the crystalline nature of the drug. The crystalline nature of the drug was clearly demonstrated by the characteristic and significant crystallographic reflection at various scattering angles appearing at  $11.4$ ,  $15.4$ ,  $18.9$ ,  $19.2$ ,  $21.6$ ,  $24.4$ ,  $16.6$ ,  $29.1$ ,  $33.1$ ,  $34.0$  to  $2\theta$ . In the XRD diffractogram of placebo IPN beads (Fig. 6B) the signal intensities were too weak, indicating that the polymeric blend of CTG-SCMC was dispersed at the molecular level. There was no indication of the presence of DFS as it was not loaded in the placebo IPN beads. IPN beads that had been loaded with DFS showed almost same reflections at the same  $2\theta$  degree angle as the XRD diffractogram of DFS (Fig. 6C). The outcomes amply demonstrated that the crystallinity of DFS in drug loaded IPN beads was retained and no amorphization of the drug took place.



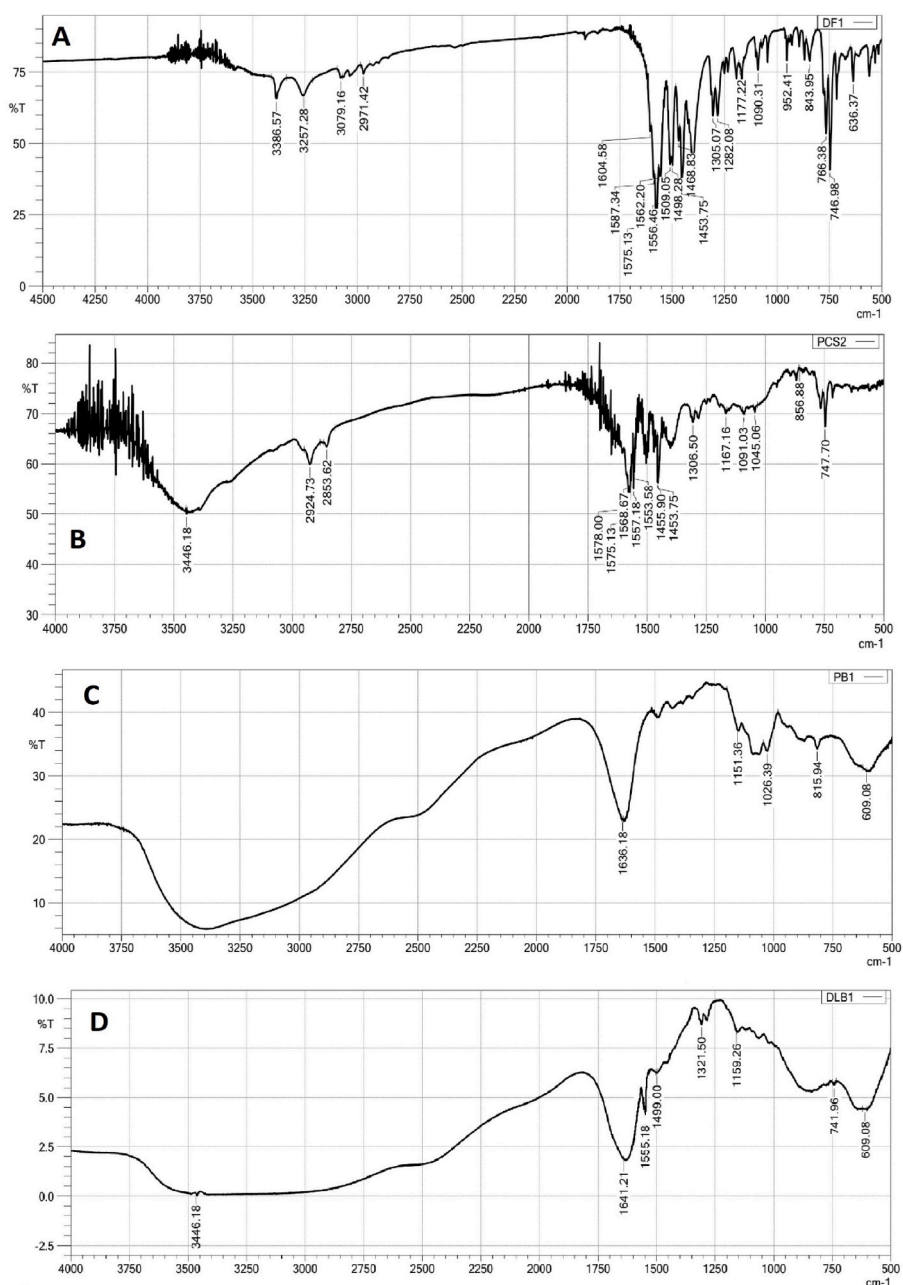


**Fig. 3.** FTIR spectra A- FTIR spectra of DFS; B- FTIR spectra of physical mixture of DFS, cassia tora gum and SCMC; C- FTIR spectra of placebo IPN beads; D- FTIR spectra of drug loaded IPN beads.

### 5.6. Production yield of IPN beads

The production yield of IPN beads is shown in Table-2. It was found in the range of 89.36%–92.76%. Results showed that factors like polymer ratio, crosslinker concentration and gelation time did not significantly affect production yield.

### 5.7. Size analysis of IPN beads

The prepared IPN beads exhibited a narrow and mono-modal particle size distribution. The size of IPN beads was found to be in the range of  $215 \pm 0.14$  to  $485 \pm 0.20 \mu\text{m}$  as shown in Table-2. It was noticed that the polymer ratio, crosslinker concentration, and gelation time had an impact on the size of the IPN beads. It was observed that when the SCMC content of the polymer blend increased, so did the size of the IPN beads. This can be explained by the hydrodynamic viscosity concept, which

states that increasing the proportion of SCMC in the polymer ratio increases the viscosity of the polymer inside the polymer droplets. Because of this, there are fewer free sites available for crosslinking, which results in an increase in the size of IPN beads [21].

The crosslinker concentration and gelation time both had a similar impact on the size of IPN beads. IPN beads shrank in size as gelation time and crosslinker concentration was increased. This is explained by the fact that when the blended polymer gel comes into contact with the  $\text{Al}^{+++}$  ions present in the crosslinking solution, an influx of  $\text{Al}^{+++}$  ions from the solution to the inside of the droplet and an efflux of water from the droplet to the outside solution take place, causing the gel layer to move inward. Increased gelation time and crosslinking concentration will lead to a greater influx of  $\text{Al}^{+++}$  ions inside the droplet, resulting in more squeezing out of water that leads to the contraction of beads and a decrease in IPN bead size. Nearly similar results were reported by Hosney et al., in 1998 [22]. This implies that throughout the

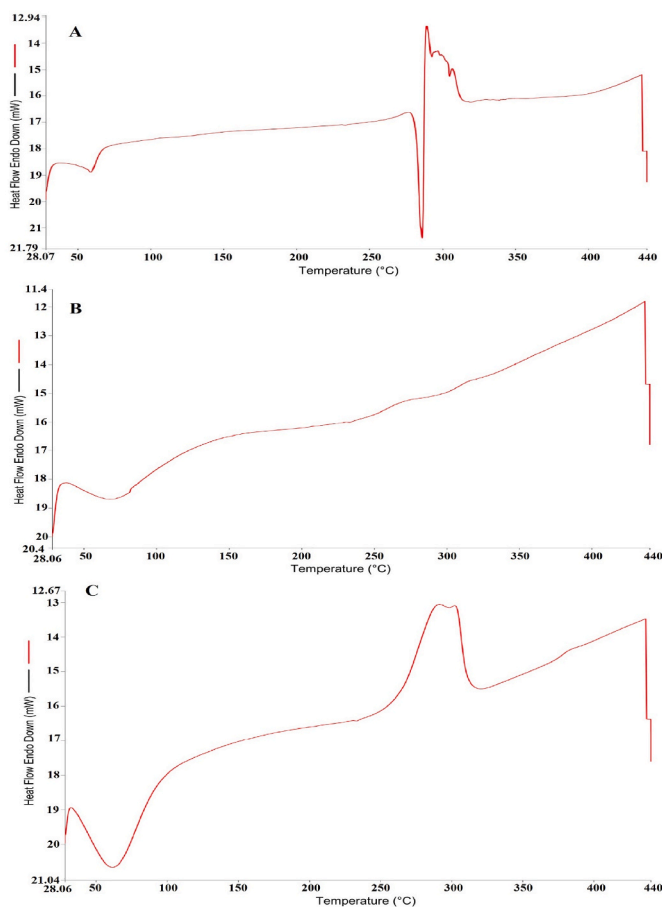


Fig. 4. DSC thermogram, A- DSC thermogram of Drug; B- DSC thermogram of cassia tora gum; C- DSC thermogram of SCMC.

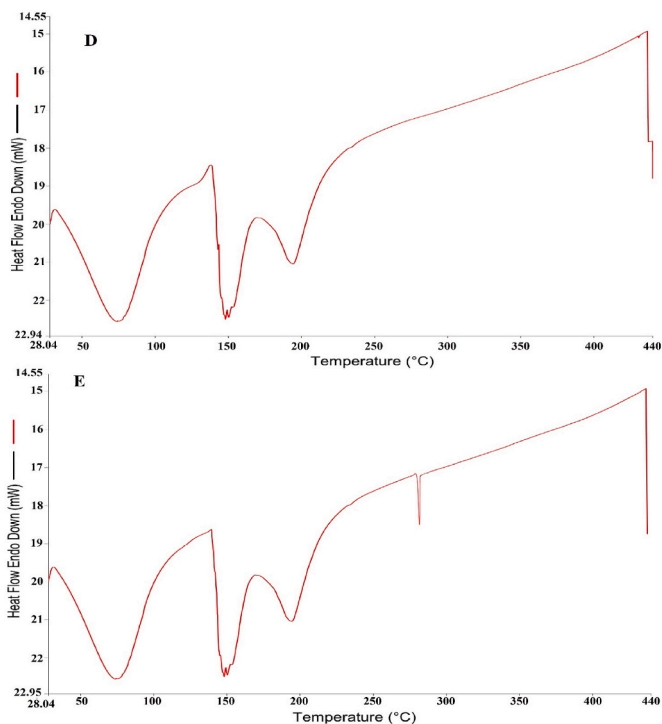


Fig. 5. DSC thermogram, D- DSC thermogram of placebo IPN beads; E- DSC thermogram of drug loaded IPN beads.

crosslinking process, the polymeric network shrank rapidly, which causes the formation of smaller, more rigid IPN beads at higher crosslinker concentration.

### 5.8. Scanning electron microscopy (SEM)

The results of SEM are shown in Fig. 7. The effect of  $AlCl_3$  concentration and gelation time was closely monitored. Photos taken during the scanning electron microscopy show that the IPN beads become more spherical as the crosslinking ion ( $Al^{+++}$ ) concentration rises. This might be explained by the fact that, as soon as the polymer blend droplets came into contact with the  $Al^{+++}$  ions in solution, the polymer droplets quickly crosslinked to produce spherical IPN beads. This reaction would have occurred quickly, resulting in the spherical shape of IPN beads. The surface morphology of IPN beads showed that the surface stiffens with increasing crosslinker concentration (Fig. 7; A3 and A6). The gelation time also had an influence on shape and surface morphology of IPN beads. The surface of the IPN beads became stiffer as gelation time increased (Fig. 7; A1, A6 and A9). The beads had a spherical shape and a smooth, wrinkle-free surface. Because of the high rigidity, low water evaporated while drying, resulting of low surface folding and wrinkles.

### 5.9. Drug entrapment efficiency

The results of the drug entrapment efficiency of IPN beads are summarized in Table-2, which ranged from  $79.50 \pm 1.69\%$  to  $91.42 \pm 1.99\%$ . The effect of all the variables (polymer ratio, crosslinker concentration, and gelation time) on drug entrapment efficiency was clearly visible. It was found that a higher degree of crosslinking results in a higher rigidification of the IPN network, which reduces the likelihood of drug leaching out during the formation of the IPN matrix structure and causes the retention of more drug particles into the core of the IPN bead, resulting in an increase in drug entrapment efficiency.

A higher amount of SCMC caused a decrease in drug entrapment efficiency. This might be because higher solubility of SCMC leads to the creation of a loose polymer matrix and higher swelling of an IPN bead during the gelation process in the crosslinker solution, which causes drug particles to leach out of the interpenetrating polymer matrix and reduces drug entrapment efficiency. A longer gelation time also reduces the drug entrapment efficiency because longer gelation times lead to increased  $Al^{+++}$  ion diffusion inside IPN beads, which displaces free drugs and reduces drug entrapment.

### 5.10. Swelling behaviour of IPN beads

The swelling ability of the IPN matrix was determined to study the release of the drug from the IPN bead. The water absorption capability of IPN beads was evaluated to identify their swelling behaviour at a pre-determined time-interval. The swelling results are shown in Table-2. The swelling behaviour of IPN beads was determined in acidic (pH 1.2) and alkaline (pH 7.4) media. Results showed that the swelling ability of IPN beads was low in acidic media and high in alkaline media. The swelling efficiency of IPN beads in acidic pH ranged from  $122.34 \pm 1.22\%$  to  $210.56 \pm 1.04\%$  and in higher pH ranged from  $299.16 \pm 1.80\%$  to  $518.34 \pm 1.98\%$ . The  $-OH$  and  $-COOH$  groups were the primary functional groups in CTG and SCMC respectively, that underwent crosslinking with  $Al^{+++}$  ions. In an acidic media (pH 1.2), these groups continue to be protonated and exert a moderate electrostatic repulsive force, which causes the beads to swell to a much lesser extent. These groups become ionised at higher pH levels (in alkaline media), which causes electrostatic repulsion between ionised groups and lengthens the distance between polymeric chains. This makes it easier for more water to be absorbed, leading to higher swelling. Furthermore, as a result of ionization, the concentration of counterions inside the interpenetrating polymeric network becomes high and a difference in osmotic pressure exists between the external and internal solutions of the IPN bead. The

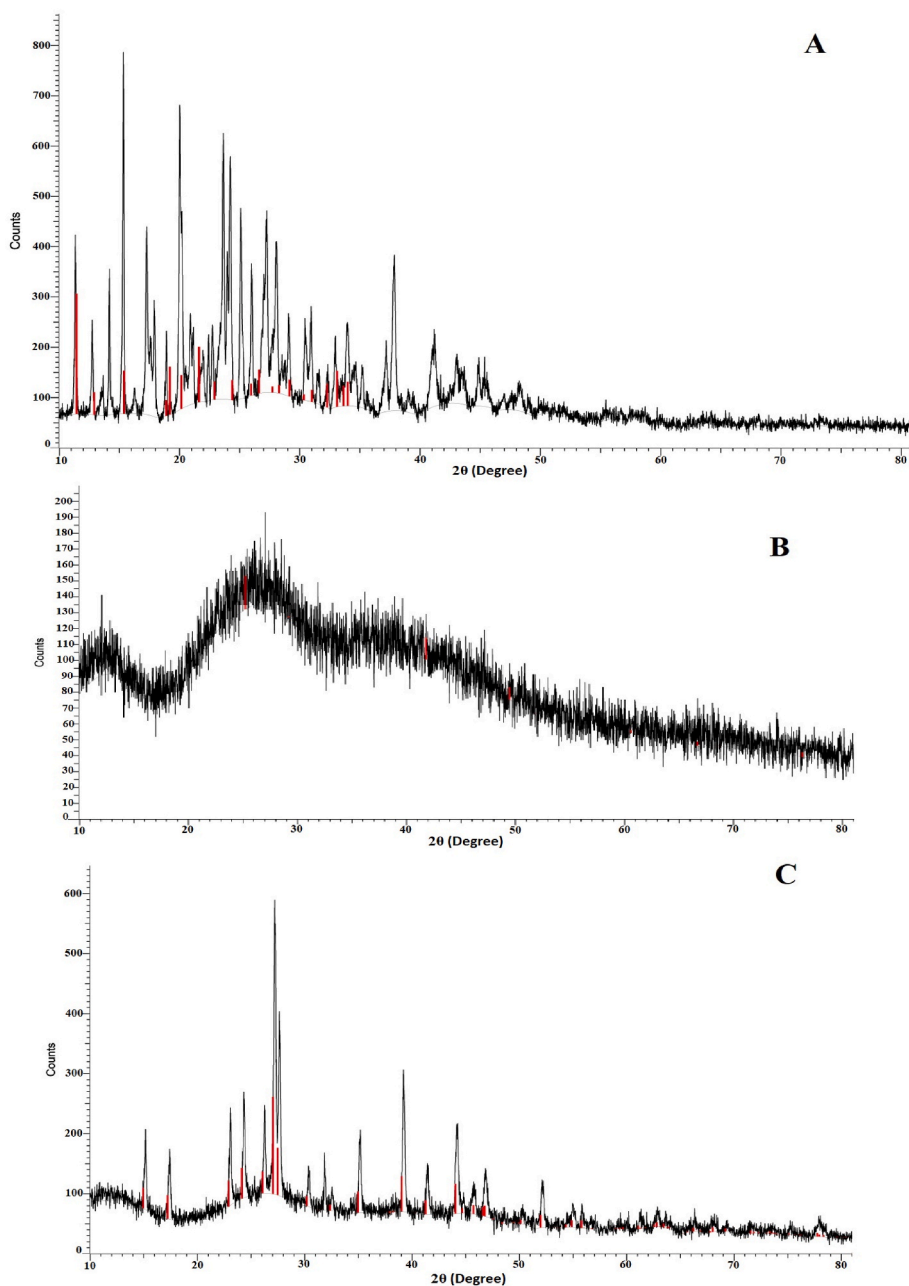


**Fig. 6.** X-ray diffraction (XRD) analysis, A- X-ray Diffractogram of Drug; B- X-ray diffractogram of placebo IPN beads; C- X-ray diffractogram of drug loaded IPN beads.

swelling of the beads balanced the increasing osmotic pressure.

From the results, it was observed that the swelling of IPN beads was indirectly proportional to the concentration of crosslinker. Swelling of IPN beads was observed to be high at low concentrations of crosslinker (4%w/v) and low at high concentrations of crosslinker (6%w/v). This is because mobility in crosslinked polymeric chains is spurred on by the swelling of IPN beads. Since  $Al^{+++}$  ions are responsible for the cross-linking of polymeric chains, at high concentration the polymer network density increases, resulting in the formation of a highly rigid and stable polymer network with reduced mobility that shows a slower tendency to swell. Similar findings were reported by Hezaveh et al., when genipin was used as a crosslinking agent [23]. From the observations, it was noted that an increase in gelation time reduces the extent of swelling. This might result from the matrix's pore volume shrinking as gelation time increases.

#### 5.11. Drug release, kinetics and mechanism study

IPN beads were used to study the release of the drug, which was first done in an acidic media (pH 1.2) for the initial 2 h and then in alkaline media (phosphate buffer pH 7.4). The graph of cumulative drug release (%) vs. time (hrs) is presented in Fig. 8. The results revealed that the drug release was very low in acidic media but as the pH of the media increased to 7.4 the release of drug from IPN beads increased significantly. In both the dissolution media, the IPN beads containing a low concentration of crosslinking agent (4%w/v) showed high drug release in comparison to the IPN beads containing a high concentration of crosslinker (6%w/v). A similar effect was observed with gelation time. This is because high concentration of crosslinker or gelation time causes high rigidization of polymer network, resulting in slow drug release.

Data on drug release kinetic modelling are given in Table-3. The IPN bead formulations followed zero order release kinetics, and the results

**Table 2**

Results of Production yield, arithmetic mean diameter, drug entrapment efficiency and equilibrium swelling of IPN beads.

Formulation Code	Production yield (%)	Arithmetic mean diameter (µm) ±SD	Entrapment efficiency (%)	Equilibrium swelling (%) ±SD	
				pH1.2	pH7.4
A1	89.36	320 ± 0.12	85.20 ± 1.62	160.20 ± 1.62	432.13 ± 2.52
A2	89.45	412 ± 0.16	80.46 ± 1.02	180.42 ± 1.32	492.65 ± 1.95
A3	90.26	485 ± 0.20	79.50 ± 1.69	210.56 ± 1.04	518.34 ± 1.98
A4	90.48	275 ± 0.18	91.42 ± 1.99	140.36 ± 1.02	302.15 ± 2.00
A5	90.20	382 ± 0.10	89.62 ± 0.97	162.42 ± 1.02	389.82 ± 1.96
A6	91.23	420 ± 0.24	86.62 ± 1.00	182.75 ± 1.69	482.25 ± 1.80
A7	92.76	215 ± 0.14	88.40 ± 1.45	122.34 ± 1.22	299.16 ± 1.80
A8	92.45	308 ± 0.12	86.62 ± 1.32	152.13 ± 1.56	322.63 ± 1.94
A9	90.67	346 ± 0.20	84.62 ± 1.78	168.30 ± 1.85	415.24 ± 1.90

suggested that the drug release rate was independent of the

concentration of dissolved species. The Korsmeyer-Peppas equation's estimated value of "n" was in the range of 0.890–0.985, indicating that the drug release mechanism from IPN beads was non-Fickian release kinetics. It relates the drug transport mechanism to stresses and state-transitions in polymers that swell when exposed to water or biological fluids. Disentanglement and erosion of polymers are also included in this term [24].

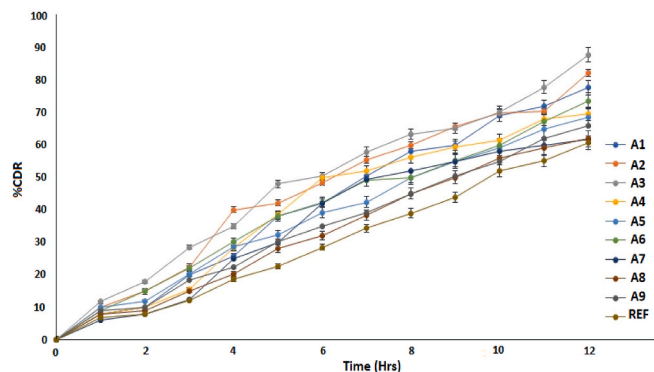


**Fig. 8.** DFS release profiles of drug loaded IPN beads in acidic media (pH 1.2) For initial 2 h and then in alkaline media (pH 7.4).

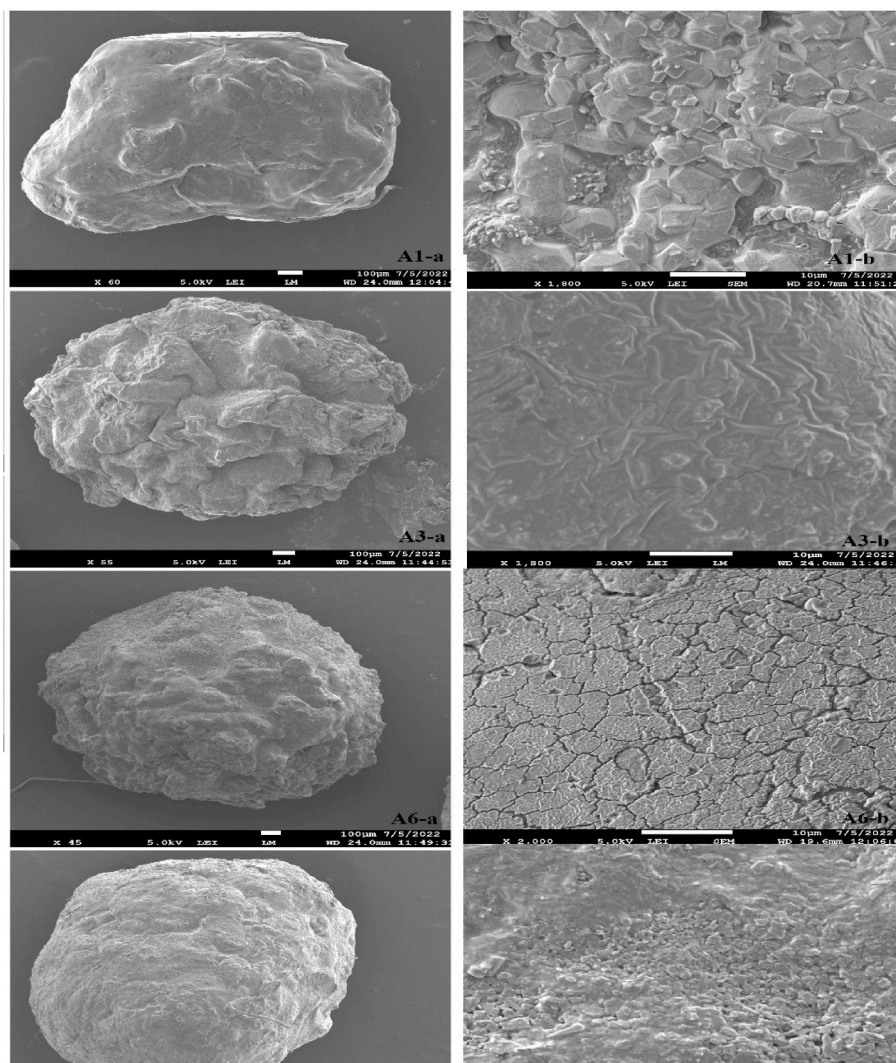


**Fig. 7.** SEM analysis of IPN beads. Key-concentration of AlCl<sub>3</sub> 4%w/v (A1, A3), 6%w/v (A6); Gelation time 30min (A1, A3), 60min (A9).



Table 3

Kinetic modelling and mechanism of drug release data.

Formulation Code	Zero order (R <sup>2</sup> )	First order (R <sup>2</sup> )	Higuchi (R <sup>2</sup> )	Korsmeyer-Peppas	
				(R <sup>2</sup> )	(n)
A1	0.990	0.977	0.927	0.976	0.949
A2	0.981	0.966	0.952	0.977	0.985
A3	0.990	0.931	0.959	0.979	0.895
A4	0.982	0.956	0.928	0.953	0.893
A5	0.993	0.987	0.945	0.980	0.927
A6	0.994	0.977	0.955	0.986	0.950
A7	0.985	0.974	0.914	0.956	0.899
A8	0.994	0.974	0.918	0.969	0.892
A9	0.996	0.979	0.928	0.972	0.890

The dissolution profiles of all the formulations were also compared by calculating two factors, f1 (difference factor) and f2 (similarity factor). According to the FDA The f1 value is equal to zero when the test and reference profiles are identical and increases as the two profiles become less similar. The f2 value between 50 and 100 is considered significantly similar. f2 factor 100 indicates that two processes are the same. The f2 values were found to be 42.86, 37.42, 34.46, 44.28, 52.71, 46.94, 53.44, 69.88, 62.96 and f1 values were 39.04, 52.26, 60.76, 35.31, 26.26, 34.03, 20.28, 10.73, 15.87 for the formulations A1 to A9 respectively. Results indicated that for formulations A8 and A9, the f1 value was near to zero (10.73, 15.87) and the f2 value was close to 100 (69.88, 62.96) respectively, among all other formulations.

## 6. Conclusion

Polymers have facilitated the development of innovative drug delivery systems by allowing therapeutic agents to be released in a controlled dose over an extended period of time, delivering the drug to specific sites, and improving stability. IPN, a novel class of polymers based on the mixing of natural and/or synthetic polymers, either alone or in combinations. The IPN beads were successfully developed by using CTG, SCMC and AlCl<sub>3</sub> (crosslinking agent) to encapsulate DFS as a model drug. The IPN beads were characterized by FTIR, DSC, XRD and SEM analysis and tested for size, encapsulation efficiency, swelling behavior, and drug release. FTIR analysis confirmed the stability of the drug in an interpenetrating polymer network. The DSC and XRD analysis revealed that the drug was present in crystalline form in the interpenetrating polymer matrix. The IPN beads were almost spherical in shape and the size ranged between 196 ± 0.22 to 0.548 ± 0.45 mm. Swelling efficiency ranged from 122.34 ± 1.22% to 210.56 ± 1.04% in acidic pH and from 299.16 ± 1.80% to 518.34 ± 1.98% at higher pH. IPN beads showed extremely minimal drug release in an acidic media but a relatively high and sustained drug release profile in alkaline pH. Results showed that the ratio of polymer, concentration of crosslinking agent and gelation time have influenced IPN bead size, encapsulation of drug, swelling of beads and drug release in different ways. The results imply that DFS-loaded IPN beads may be used to lessen the drug's release in an acidic medium and to alter the drug's release in an alkaline medium, thus minimizing the gastric adverse effects of DFS.

## Credit author statement

Alka Lohani: Conceptualization, Methodology, Writing- Original draft preparation, Investigation.

Mohit Maurya: Visualization, Investigation.

Sushil Kumar: Supervision, Writing- Reviewing and Editing.

Navneet Verma: Supervision, Writing- Reviewing and Editing.

## Funding

No funding was received for this work.

## Declaration of competing interest

The authors declare no conflict of interest.

## Data availability

No data was used for the research described in the article.

## Acknowledgement

The authors are grateful to the Vice Chancellor, IFTM University, Moradabad for providing necessary facilities for this research work, SAIF, Birbal Sahni Institute of Palaeosciences, Lucknow, India for SEM facility and Central Instrumentation Facility, Lovely Professional University Punjab for XRD and DSC facility.

## References

- [1] K.E. Urich, S.M. Cannizzaro, R.S. Langer, K.M. Shakesheff, Polymeric systems for controlled drug release, *Chem. Rev.* 99 (11) (1999) 3181–3198, <https://doi.org/10.1021/CR940351U>.
- [2] O. Pillai, R. Panchagnula, Polymers in drug delivery, *Curr. Opin. Chem. Biol.* 5 (4) (2001) 447–451, [https://doi.org/10.1016/S1367-5931\(00\)00227-1](https://doi.org/10.1016/S1367-5931(00)00227-1).
- [3] D. Schmaljohann, Thermo- and pH-responsive polymers in drug delivery, *Adv. Drug Deliv. Rev.* 58 (15) (2006) 1655–1670, <https://doi.org/10.1016/j.addr.2006.09.020>.
- [4] A. Lohani, G. Singh, S.S. Bhattacharya, A. Verma, Interpenetrating polymer networks as innovative drug delivery systems, *J. Drug Deliv.* 14 (2014) 1–11, 2014.
- [5] N. Raina, R. Rani, A. Khan, K. Nagpal, M. Gupta, Interpenetrating polymer network as a pioneer drug delivery system: a review, *Polym. Bull.* 77 (9) (2019) 5027–5050, <https://doi.org/10.1007/S00289-019-02996-5>, 2019 77:9.
- [6] C. Roland, Interpenetrating polymer networks (IPN Q 1) : structure and mechanical behavior, in: S. Kobayashi, K. Müllen (Eds.), *Encyclopedia of Polymeric Nanomaterials*, Springer, Berlin, Heidelberg, 2014, [https://doi.org/10.1007/978-3-642-36199-9\\_91-1](https://doi.org/10.1007/978-3-642-36199-9_91-1).
- [7] L.H. Sperling, R. Hu, Interpenetrating polymer networks, *Polymer Blends Handbook* (2014) 677–724, [https://doi.org/10.1007/978-94-007-6064-6\\_8/COVER/](https://doi.org/10.1007/978-94-007-6064-6_8/COVER/).
- [8] B.R. Sharma, V. Kumar, P.L. Soni, Cyanoethylation of Cassia tora gum, *Starch - Stärke* 55 (1) (2003) 38–42, <https://doi.org/10.1002/STAR.200390004>.
- [9] F.J. Rodrigues, M.F. Cedran, G.A. Pereira, J.L. Bicas, H.H. Sato, Effective encapsulation of reuterin-producing *Limosilactobacillus reuteri* in alginate beads prepared with different mucilages/gums, *Biotechnol. Rep.* 34 (2022), e00737, <https://doi.org/10.1016/J.BTRE.2022.E00737>.
- [10] H.A. Pawar, P.M. Mello, Spectrophotometric estimation of total polysaccharides in Cassia tora gum, *J. Appl. Pharmaceut. Sci.* (2011) 93–95, 03.
- [11] X.H. Yang, W.L. Zhu, Viscosity properties of sodium carboxymethylcellulose solutions, *Cellulose* 14 (5) (2007) 409–417, <https://doi.org/10.1007/S10570-007-9137-9>, 2007 14:5.
- [12] A.A. Oun, J.W. Rhim, Preparation and characterization of sodium carboxymethyl cellulose/cotton linter cellulose nanofibril composite films, *Carbohydr. Polym.* 127 (2015) 101–109, <https://doi.org/10.1016/j.carbpol.2015.03.073>.
- [13] T. Reddy, S. Tammishetti, Gastric resistant microbeads of metal ion cross-linked carboxymethyl guar gum for oral drug delivery, Gastric resistant microbeads of metal ion cross-linked carboxymethyl guar gum for oral drug delivery 19 (3) (2008) 311–318, <https://doi.org/10.1080/02652040110081389>.
- [14] R.N. Brogden, R.C. Heel, G.E. Pakes, T.M. Speight, G.S. Avery, Diclofenac sodium: a review of its pharmacological properties and therapeutic use in rheumatic diseases and pain of varying origin, *Drugs* 20 (1) (1980) 24–48, <https://doi.org/10.2165/00003495-198020010-00002>.
- [15] S. Muhammad, F. Hasan, S.M. Farid Hasan, T. Ahmed, N. Talib, F. Hasan, Pharmacokinetics of diclofenac sodium in normal man, *Pak. J. Pharm. Sci.* 18 (1) (2005) 18–24.
- [16] B.M. Al-Taani, B.M. Tashtoush, Effect of microenvironment pH of swellable and erodible buffered matrices on the release characteristics of diclofenac sodium, *AAPS PharmSciTech* 4 (3) (2003) 110–115, <https://doi.org/10.1208/pt040343>.
- [17] R.S. Devi, S. Narayan, G. Vani, C.S.S. Devi, Gastroprotective effect of Terminalia arjuna bark on diclofenac sodium induced gastric ulcer, *Chem. Biol. Interact.* 167 (1) (2007) 71–83, <https://doi.org/10.1016/J.CBI.2007.01.011>.
- [18] S.S. Bhattacharya, A.K. Ghosh, S. Banerjee, P. Chattopadhyay, A. Ghosh, Al<sup>3+</sup> ion cross-linked interpenetrating polymeric network microbeads from tailored natural polysaccharides, *Int. J. Biol. Macromol.* 51 (5) (2012) 1173–1184, <https://doi.org/10.1016/j.ijbiomac.2012.08.029>.
- [19] S. Ray, S. Banerjee, S. Maiti, B. Laha, S. Barik, B. Sa, U.K. Bhattacharyya, Novel interpenetrating network microspheres of xanthan gum–poly(vinyl alcohol) for the delivery of diclofenac sodium to the intestine—in vitro and in vivo evaluation 17 (7) (2010) 508–519, <https://doi.org/10.3109/10717544.2010.483256>.
- [20] M. Rani, A. Agarwal, Y.S. Negi, Characterization and biodegradation studies for interpenetrating polymeric network (IPN) of chitosan-amino acid beads, *J. Biomaterials Nanobiotechnol.* (2011) 71–84, <https://doi.org/10.4236/JBNB.2011.21010>, 02(01).

- [21] A. Lohani, G. Singh, S.S. Bhattacharya, R. Hegde, A. Verma, Tailored-interpenetrating polymer network beads of  $\kappa$ -carrageenan and sodium carboxymethyl cellulose for controlled drug delivery, *J. Drug Deliv. Sci. Technol.* 1 (31) (2016) 53–64.
- [22] E.A. Hosny, A.A.R.M. Al-Helw, Effect of coating of aluminum carboxymethylcellulose beads on the release and bioavailability of diclofenac sodium, *Pharm. Acta Helv.* 72 (5) (1998) 255–261, [https://doi.org/10.1016/S0031-6865\(97\)00040-X](https://doi.org/10.1016/S0031-6865(97)00040-X).
- [23] H. Hezaveh, I.I. Muhamad, I. Noshadi, L. Shu Fen, N. Ngadi, Swelling behaviour and controlled drug release from cross-linked  $\kappa$ -carrageenan/NaCMC hydrogel by diffusion mechanism, *J. Microencapsul.* 29 (4) (2012) 368–379, <https://doi.org/10.3109/02652048.2011.651501>.
- [24] M.P. Paarakh, P.A. Jose, C.M. Setty, G.P. Christopher, Release kinetics–concepts and applications, *Int. J. Pharm. Res. Technol.* 8 (1) (2018) 12–20.